proceedings

MDPI

Synthesis and Characterization of Graphene-oxide Reinforced Copper Matrix Composite[†]

Isaque Moura 1 *, **Talita Sousa 1, Andreza Lima 1 Wesley Oliveira 1 and Luiz Brandão 1**

[1] Instituto Militar de Engenharia, Seção de Ciência dos Materiais SE/8, Rio de Janeiro Instituto Militar de Engenharia, Brazil; isaquebrito@ime.eb.br (I.M.), talitagama@ime.eb.br (T.G.), andrezamenezeslima@gmail.com (A.M.), oliveira.dje@gmail.com (W.O.) and brandao@ime.eb.br (L.P.)

[*] Correspondence: isaquebrito@ime.eb.br.

[†] Presented at the 2nd International Online-Conference on Nanomaterials, 15–30 November 2020; Available online: https://iocn2020.sciforum.net/.

Abstract: In this study, eletrolitical copper powder (Cu) was initially mixed with the aqueous solution of graphene oxide (GO), later the mixture underwent mechanical stirring for 1 hour, vacuum filtration and drying for 42 hours. The final concentration of GO in the composite was 0.3%wt. Through scanning electron microscopy (SEM), it was possible to observe the homogeneous dispersion of graphene sheets between copper particles, without the presence of agglomerates. In addition, the X-ray diffraction (XRD) of the pure samples and after mixing, revealed that there was no oxidation of the copper and absence of peaks related to other elements, confirming the high purity of the copper used. Still by XRD it was possible to analyze that the graphene oxide produced was formed by stacking layers of graphene due to the appearance of a diffraction peak referring to the plane (002), which was confirmed by Raman Spectroscopy performed in GO from the appearance of the 2D bands. Fourier transform infrared spectroscopy (FTIR) allowed the identification of the vibrational spectra referring to the hydroxyl, carbonyl and epoxy functional groups in GO, confirming that the oxidation process was effective in inserting functional groups in the basal graphical plane. Through the GO thermogravimetric analysis (TGA) it was possible to identify a significant loss of mass of approximately 30% at temperatures below 100 °C, referring to the elimination of water molecules, the most stable functional groups were eliminated at temperatures between 600 °C and 800 °C.

Keywords: Graphene oxide; copper; TGA; FTIR; SEM

1. Introduction

The interest in the study and development of routes to increase copper resistance has received special attention from researchers in recent years [1,2], especially the formation of composites with different types of addition of reinforcement material. This is due to this method having been effective in improving its mechanical properties, interfering less significantly in the electrical conductivity [3–5]. In this prerogative, carbon-based materials, when used as reinforcements, increase the strength of the matrix without much compromising the electrical conductivity of the composite [7]. One of the factors that explains this characteristic is the low solubility between copper and carbon, making the diffusion of the carbonaceous material in the copper matrix very low [7,8]. Due to its superior characteristics to other materials, graphene and its derivatives have been studied for incorporation in these composites, showing high values of mechanical resistance and electrical conductivity. Graphene is a planar carbon monolayer whose atoms are arranged in a two-dimensional form (2D) and is considered the most resistant material ever tested, obtaining tensile strength values of 130 GPa [9,10]. In addition, it has high values of electrical ($\sigma = 10^6$ Ωcm^{-1}) and thermal conductivity (5000 Wm^{-}

[1] K^{-1}) [11,12]. Graphene oxide (GO) is the main derivative of graphene and its structure contains many oxygen-containing functional groups e.g. epoxy, hydroxyls, carbonyls and carboxyls linked to the layer of carbon atoms [13]. The manufacture of copper-graphene composites has been studied through the use of several manufacturing techniques and different attempts to determine processing parameters. Among them the obtaining of an optimized dispersion of graphene in the matrix, favoring a good adhesion between the components and an attempt to minimize the agglomeration of graphene between grain boundaries, the latter has been one of the greatest challenges [14,16]. The analysis of powders is essential due to the need to understand the changes that materials can undergo in their properties when performed different processes [17]. For a better understanding of the final properties of the composite in this study, thermal and microstructural analysis of Cu-Gr powders were performed, presented in a systematic manner below.

2. Materials and Methods

2.1. Preparation of Cu/GO composite

The GO used in this study was produced by liquid-phase exfoliation (LPE), based on the method of Hummers and Offeman (1958) [18] and modified by Rourke et al. (2011) [19]. This method allows to obtain GO sheets with a great superficial extension and a large amount of oxidized functional groups, which in turn facilitate the adhesion of nanoparticulate materials on its surface. Pure copper powder (Cu) with a purity of 99.94% and Graphene oxide with a concentration of 4.55 mg/mL were mixed by mechanical stirring for 1 h. The chemical composition of the composite was 0.3%wt GO. Vacuum filtration using kitassato and Buncher funnel was performed followed by vacuum drying for 42 h in order to obtain the dry powder.

2.2. Characterization

The morphologies of Copper and Cu/GO composite powders were observed by scanning electron microscopy (SEM, FEI Quanta FEG 250). X-Ray Diffraction (XRD, PANalytical X Pert Pro MRD) was performed with Co Ka radiation and operated at 40 kV and 40 mA. Raman spectra (NT-MDT NTEGRA Spectra) was perfomed on GO in order to observe the bands D and G, the wavelength of the laser used was 473 nm with a scanning range between 702 and 3343 cm^{-1}, and an exposure time of 200 s. Thermogravimetric analysis (TGA, TGA Q-500 equipment) and Fourier transform infrared (FTIR, Perkin Elmer FT-IR/FIR spectrometer with ATR accessory) were performed on GO and Cu/GO composites, for TGA analyses the samples were analyzed up to 800 °C, in a controlled atmosphere of nitrogen, with a heating rate of 10 °C/min and FTIR was taken with number of scans 60 and 4 cm^{-1} resolution.

3. Results and Discussion

3.1. Powders and GO morphology and microstructural analysis

In Figure 1 (a) and (b) the SEM images of the pure copper powder are presented, the granulometric distribution has a wide range and in general it can be seen that the particles have an irregular shape, being constituted by clusters of smaller particles, as is possible note, specifically, in the image of Figure 1 (b). The particle shape and sizes are consistent with the electrolytic manufacturing process used, which gives rise to irregular or dendritic particles with an average particle size between 5 and 300 mm calculated by Faria et al. [21]. In Figure 1 (c) and (d) the images of the copper-graphene composite are presented, in which the particles resemble the aspect of the pure copper powder, presented in Figure 1 (a). It is possible to identify the GO sheets adhered to the surface of the copper particles and between the particles, showing adhesion between the copper and the GO.
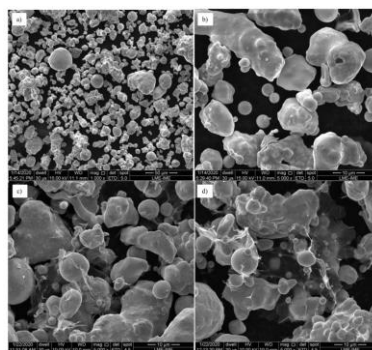
Figure 1. SEM (a,b) pure copper; (c,d) composite Cu/GO.

Figure 2 (a) shows the diffractogram obtained for graphene oxide. Through the synthesis used we have the generation of few layers of graphene, being possible to obtain a sharp diffraction peak in the diffractogram start. The identified peak refers to the plane (002), related to the HC structure of carbon. The diffraction peaks shown in the diffractogram refer to the leaves that are not arranged in the form of monolayers, as monolayers do not show a diffraction peak. Thus, together with the production method, there is an indication that the GO used for this study is formed by several layers. By Figure 2 (a) one can notice a decrease in the diffraction angle in relation to pure graphite, used for GO production, attributed to the increase in GO interplanar distances due to the insertion of functional groups during oxidation and the possibility of the presence of water molecules between the layers [20]. Figure 2 (b) shows the diffractogram obtained for the pure copper powder and for composite Cu/GO, the peaks referring to the planes (111), (200), (220), (311) and (222). These plans refer to the FCC structure of copper and no other peak was indexed, ensuring that the copper powder did not have other elements or oxidation, or the present oxidation resulted in a very small amount of oxide, being insufficient to generate a peak above the noise of the diffractogram. In addition, no peak was observed for the GO, this is due to the concentration used to manufacture the composite being so low that it does not generate a diffraction peak.
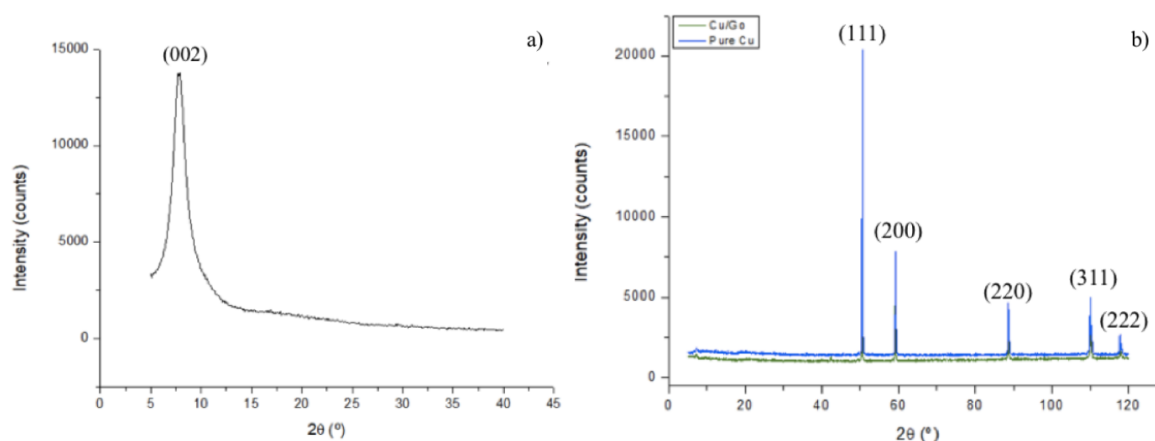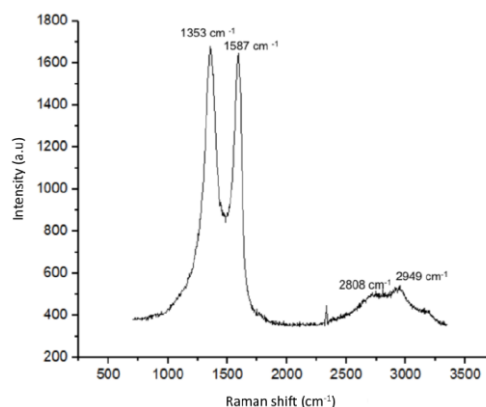

Figure 2. XRD of (a) GO; (b) Pure copper and Cu/GO composite.

3.2. Spectroscopy

3.2.1. Raman Analysis

Raman spectroscopy was performed on the dispersion of graphene oxide used for the manufacture of the powdered composite. In Figure 3 presents the Raman spectra found for the GO.

Figure 3. Raman spectra of GO used.

The Raman Spectra of graphene normally shows peaks referring to the D (~ 1350 cm^{-1}) and G (~ 1580 cm^{-1}) bands. In this study were found bands D (1353 cm^{-1}) and G (1587 cm^{-1}) with Raman displacement similar to those found in the works of Faria et al. [21], Yue et al. [22] and Gao et al. [23]. The relationship between the intensities of bands D and G allows to obtain the amount of defects present in the carbon structure. The ID/IG ratio for GO is greater than that of graphene and reduced graphene oxide and this is due to the presence of oxygenated functional groups linked to the carbon structure [15]. The ratio of the intensities of bands D and G used in this study was approximately 1.0. In addition to the bands D and G, it was possible to observe the presence of the peaks referring to the bands 2D (2808 cm^{-1}) and 2D' (2949 cm^{-1}). These bands appear with less intensity in relation to the D and G bands and are related to the stacking of a number of carbon layers of the graphene structure [24]. Thus, the presence of these bands shows that the oxide analyzed is formed by stacking layers and not just monolayers, which can be confirmed by the X-Ray Diffraction analysis presented in Figure 2 (a).

### 3.2.2. Fourier Transform Infrared Spectroscopy

Fourier transform infrared spectroscopy (FTIR) was obtained at the Instrumental Support Laboratory (LAPIN1) of the Institute of Macromolecules Professora Eloisa Mano (IMA-UFRJ). The analysis of the spectrum obtained for GO (Figure 4 (a)) allows us to initially observe the occurrence of a broadband between 3000 to 3700 cm^{-1}, which is related to the existence of water adsorbed between the leaves and a peak at 3347 cm^{-1}, which can be attributed the OH stretching range. At 1626 cm^{-1} another peak is identified, corresponding to the stretching vibrations of C=O; followed by a third peak at 1158 cm^{-1}, referring to vibrations of C-O-C epoxy groups; 1036 cm^{-1}, vibrations of C-OH bonds and finally a last peak at 873 cm^{-1}, due to the stretching vibrations of epoxy groups [25–27]. For composite Cu/GO presents in Figure 4 (b) some characteristic peaks can be observed relative to the GO, presented in Figure 4 (a), such as the existence of a band present in approximately 3500 cm^{-1}, related to the O-H elongation vibration. The absorption bands observed at 2954 cm^{-1} can correspond to symmetric vibration of C-H bond. At 1060 cm^{-1}, a band related to C-O elongation (epoxy/ether) is noted. A peak appeared at 596 cm^{-1}, which is attributed to observation of hydroxyl deformation modes [15,28,29].
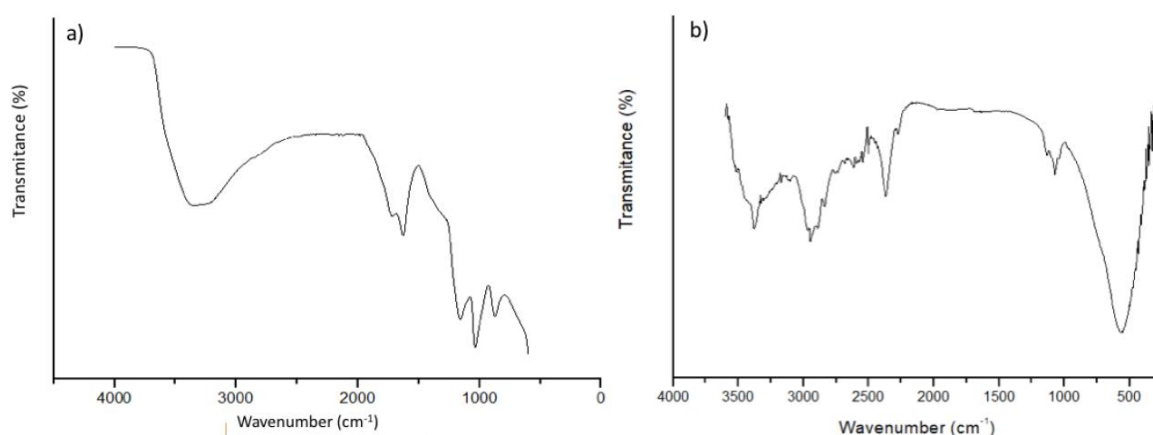
Figure 4. FTIR spectra of (a) GO; (b) Cu/GO composite**.**

3.3. Thermogravimetric Analysis

Thermal analysiswere performed on GO and composite powder in order to verify the effectiveness of the method of mechanical stirring, filtration and vacuum drying. The thermogravimetric analysis (TGA) is seen in Figure 5, and was also obtained at LAPIN1 (IMA-UFRJ).
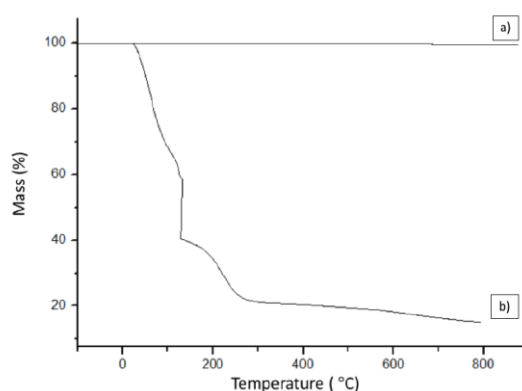
Figure 5. TGA of (a) Cu/GO composite and (b) GO.

For the composite (Figure 5 (a)) it is possible to notice that there is no change in mass as there was no gain its possible to deduce that there was no oxidation and the fact that there is no loss of weight is due to the low amount of graphene in the composite, being formed mainly of copper [30]. For GO (Figure 5 (b)) it is possible to initially observe a loss of mass below 100 °C, of about 30%, which is associated with the elimination of adsorbed water and gas molecules. The range between 100-200 °C shows an abrupt loss of 34% in mass and between 200-300 °C of 13%, which are related to the elimination of functional oxygen groups. In the region of 300-600 °C the material remains stable, showing a small loss of mass (approximately 3%), followed by a last loss in the region of 600-800 °C, related to the removal of functional oxygen groups even more stable [25,26].

4. Conclusions

In conclusion, copper-graphene composites were synthetized by mechanical stirring. Based on the results obtained by SEM and XRD, it is suggested that uniform mixtures of GO between the copper particles were obtained so that there were no large agglomerates, showing that the mixing method through the mechanical stirring of the powder in aqueous dispersion was efficient to obtain the composite powder with good homogeneity and no oxidation. The GO used was formed by several layers, which was confirmed by the presence of 2D bands in Raman spectra.

References

1. SOUSA, T. G.; MOURA, I. A. B.; FILHO, F. C. G.; MONTEIRO, S. N.; BRANDÃO, L. P. Combining severe plastic deformation and precipitation to enhance mechanical strength and electrical conductivity of Cu–0.65Cr–0.08Zr alloy. *Journal of Materials Research and Technology* **2020**, *9*, 5953–5961.

2. MENG, A.; NIE, J.;WEI, K. et al. Optimization of strength, ductility and electrical conductivity of a Cu–Cr–Zr alloy by cold rolling and aging treatment. *Vacuum* **2019**, *167*, 329–335.

3. ZHOU et al. The effects of graphene content on the corrosion resistance, and electrical, termal andmechanical properties of graphene/copper composites. *New Carbon Materials* **2019**, *787*, 786–793.

4. MOGHANIAN, A.; SHARIFIANJAZI, F.; ABACHI, P. et al. Production and properties of Cu/TiO2 nano-composites. *Journal Alloys Compd.* **2017**, *698*, 518–524.

5. SELVAKUMAR, V. et al. Evaluation of mechanical and tribological behavior of Al-4%Cu-x%SiC composites prepared through poder metallurgy technique. *Trans. Indian Inst. Met.* **2017**, *70*, 1305–1315.

6. SINGH, V.; JOUNG, D.; ZHAI, L.; DAS, S. KHONDAKER, S. I.; SEAL, S. Graphene based material: past, present and future. *Prog. Mater. Sci.* **2011**, *56*, 1178–1271.

7. SINGH, M. et al. Annealing induced electrical conduction and band gap variation in thermally reduced graphene oxide films with different sp2/sp3 fraction. *Applied Surface Science.* **2015**, *326*, 236–242.

8. FADAVI, B, A. et al. Enhanced tensile properties of aluminium matrix composites reinforced with graphene encapsulated SiC nanoparticles. *Composites Part A: Applied Science and Manufacturing* **2015**, *68*, 155–163.

9. BALADIN, A. et al. Superior termal conductivity of single-layer graphene. *Nano Lett.* **2008**, *8*, 902–907.

10. GEIM, A. K.; NOVOSELOV, K. S. The rise of graphene. *Nature Matter* **2007**, *6*, 183.

11. NOVOSELOV, K. S. et al. Electric field effect in atomically thin carbon films *Science* **2004**, *306*, 666–669.

12. NOVOSELOV, K. S.; GEIM, A. K., MOROZOV, S. V.; et al. Two-dimensional gas of massless Dirac fermions in graphene *Nature (London).* **2005**, *438*, 197–200.

13. GAO, W.; ALEMANY, L. B.; CI, L.; AJAYAN, P. M. New insights into the structure and reduction of graphite oxide. *Nature Chemistry.* **2009**, *1*, 403–408.

14. JAGANNADHAM, K. Thermal conductivity of copper-graphene composite films synthesized by eletrochemical deposition with exfoliated graphene platelets *Metallurgical and Materials Transactions.* **2011**, *43*, 316–324.

15. HWANG, J.; YOON, T., JIN, S. H. et al. Enhancedmechanical properties of graphene/copper nanocomposites using a molecular-level mixing process. *Adv. Mater* **2013**, *25*, 6724–6729.

16. DUTKIEWICZ, J. et al. Microstructure and properties of bulk copper matrix composites strengthened with various kinds of graphene nanoplatelets. *Materials Science Engineering A.* **2015**, *628*, 124–134.

17. TIAN, Y et al. Elemental analysis of powders with surface-assisted thin film laser-induced breakdown spectroscopy. *Spectrochimia Acta Part B.* **2016**, *124*, 16–24.

18. HUMMERS,W. S.; OFFEMAN, R. E Preparation of Graphitic Oxide. **1957**, *208*, 1937–1957.

19. ROURKE, J. P.; PANDEY, P. A.; MOORE, J. J. et al. The Real Graphene Oxide Revealed: Stripping the Oxidative Debris from the Graphene-like Sheets. *Angew. Chem. Int.* **2011**, *50*, 3173–3177.

20. SWAIN, K. A. and BAHADUR, D. Enhanced Stability of Reduced Graphene Oxide Colloid Using Cross-Linking Polymers. *J. Phys. Chem. C.* **2014**, *118*, 9450–9457.

21. FARIA et al. Compósitos cobre-grafeno produzidos por metalurgia do pó com compactação a frio. 72nd *ABM Annual Congress*. **2017**, *72*, 2553–2560.

22. YUE et al. Effect of ball-milling and graphene contents on themechanical properties and fracturemechanisms of graphene nanosheets reinforced copper matrix composites. *Journal of Alloys and Compounds*. **2017**, *691*, 755–762.

23. GAO, X. et al. Mechanical properties and thermal conductivity of graphene reinforced copper matrix composites. *Powder Technology*. **2016**, *301*, 601–607.

24. FERRARI, A. C.; BASKO, D. M. Raman spectroscopy as a versatile tool for studying the properties of graphene. *Nature nanotechnology* **2013**, *8*, 235–246.

25. PRUNA, A.; PULLINI, D.; BUSQUETS, D. Influence of synthesis conditions on properties of green-reduced graphene oxide. *Journal Nanopart Res*. **2013**, *15*, 1605.

26. COROS, M. et al. Green synthesis, characterization and potential application of reduced graphene oxide. *Physica E: Low-dimensional Systems and Nanostructures*. **2020**, *119*, 113971.

27. GHADIM et al. Pulsed laser irradiation for environment friendly reduction of graphene oxide suspensions *Applied Surface Science* **2014**, *301*, 183–188.

28. LORYUENYONG, V. et al. Preparation and characterization of reduced graphene oxide sheets via water-based exfoliation and reduction methods. *Ann. Mater. Sci. Eng*. **2013**, *352*, 403–411.

29. SARKAR, C.; DOLUI, S. K. Synthesis of copper oxide/reduced graphene oxide nanocomposite and its enhanced catalytic activity towards reduction of 4- nitrophenol *RSC Adv*. **2015**, *5*, 60–72.

30. ZHANG, L. et al. In situ synthesis of three-dimensional graphene skeleton copper azide with tunable sensitivity performance. *Materials Letters*. **2020**, *279*, 128466.